Applied Physics Letters

Three-Josephson junctions flux qubit couplings

Cite as: Appl. Phys. Lett. **119**, 222601 (2021); https://doi.org/10.1063/5.0069530
Submitted: 31 August 2021 • Accepted: 10 November 2021 • Published Online: 01 December 2021

María Hita-Pérez, Gabriel Jaumà, Manuel Pino, et al.

AIP Publishing

Applied Physics Letters ARTICLE scitation.org/journal/apl

Three-Josephson junctions flux qubit couplings

Cite as: Appl. Phys. Lett. **119**, 222601 (2021); doi: 10.1063/5.0069530
Submitted: 31 August 2021 · Accepted: 10 November 2021 ·
Published Online: 1 December 2021

María Hita-Pérez,[a] Gabriel Jaumà, Manuel Pino,[b] and Juan José García-Ripoll

AFFILIATIONS

Institute of Fundamental Physics IFF-CSIC, Calle Serrano 113b, Madrid 28006, Spain

Note: This paper is part of the APL Special Collection on Emerging Qubit Systems - Novel Materials, Encodings and Architectures.
[a]**Author to whom correspondence should be addressed:** hitaperezmaria@gmail.com
[b]**Present address:** Nanotechnology Group, USAL-Nanolab, Universidad de Salamanca, E-37008 Salamanca, Spain.

ABSTRACT

We analyze the coupling of two flux qubits with a general many-body projector into the low-energy subspace. Specifically, we extract the effective Hamiltonians that controls the dynamics of two qubits when they are coupled via a capacitor and/or via a Josephson junction. While the capacitor induces a static charge coupling tunable by design, the Josephson junction produces a magnetic-like interaction easily tunable by replacing the junction with a superconducting quantum interference device. Those two elements allow to engineer qubits Hamiltonians with *XX*, *YY*, and *ZZ* interactions, including ultrastrongly coupled ones. We present an exhaustive numerical study for two three-Josephson junctions flux qubit that can be directly used in experimental work. The method developed here, namely, the numerical tool to extract qubit effective Hamiltonians at strong coupling, can be applied to replicate our analysis for general systems of many qubits and any type of coupling.

Qubit–qubit interactions are a fundamental tool for quantum information processing, both in existing quantum computers[1] and in quantum simulators.[2–4] Qubits that interact directly by physical means usually develop dipolar-like couplings with a well-defined orientation—$\sigma_1^x\sigma_2^x$ or $\sigma_1^z\sigma_2^z$ on the qubit basis—due to the electromagnetic nature of those interactions. This is the case of transmons and flux qubits, objects, which exhibit capacitive and inductive type couplings, respectively.

In recent years, there has been growing interest in enlarging the families of interactions between superconducting qubits[5–8] while preserving their strength. This has obvious advantages in the world of quantum computing by making possible the implementation of a rich family of gates.[9] It is also relevant in the development of quantum simulators, enabling nonstoquastic models that are harder to simulate classically,[6,10–13] and which could eventually lead to universal adiabatic quantum computation.[14–16] In this context, flux qubits[6–8] gain extra relevance when compared to transmon qubits.[5] The large anharmonicity of flux qubits ensures the preservation of a well-defined qubit basis even for ultrastrong couplings that dominate over the qubit's local Hamiltonian. In comparison, an ultrastrong interaction between transmon qubits enables transitions from qubit states to the weakly anharmonic excitations, so that the effective dynamics cannot be captured by a spin-1/2 model.

In this work, we perform an exhaustive study of inductive and capacitive couplings between three-Josephson-junction flux qubits (3JJQ),[17] as an alternative to the commonly used rf-superconducting quantum interference device (SQUID) qubits,[6] analyzing the origin of the interactions and the effective Hamiltonians that they produce. The capacitive interaction is implemented via a capacitor joining the two qubits, and the inductive-like coupling comes from a shared Josephson junction. One of our main goals is to determine the best circuit designs and parameter region that provides large couplings while retaining acceptable qubits properties. This is relevant in a scenario where there is a nonlinear dependence of physical properties on the circuit parameters.

We are interested in the extraction of the effective low-energy Hamiltonian for this type of interacting circuits. Our tool to do so is an improved version of the Schrieffer–Wolff transformation (SWT) introduced in Ref. 7. This method has allowed us to demonstrate that capacitively and inductively coupled 3JJQs reproduce a fairly large family of spin-1/2 models, with strong and nonstoquastic couplings on the qubit basis. If we denote the Hamiltonian of one flux qubit as $H_q = \frac{\Delta}{2}\sigma^z$, the Josephson junction coupling produces a magnetic-like interaction of the $J_{xx}\sigma_1^x\sigma_2^x$ form, while the capacitive coupling creates interactions along orthogonal directions $J_{yy}\sigma_1^y\sigma_2^y$ and $J_{zz}\sigma_1^z\sigma_2^z$.[6,7,18,19] Our study shows regimes of strong coupling with $J_{xx} \approx J_{yy} \approx J_{zz} > \Delta$ using realistic qubit designs as those proposed by Ref. 20.

We first analyze the numerical method that allows us to extract the effective Hamiltonians H_{eff} from a general many-body system by means of the SWT. A unitary mapping between two nonorthogonal

subspaces of the same dimension,[21,22] represented by projectors P_0 and P,

$$U = \sqrt{(2P_0 - \mathbb{1}_0)(2P - \mathbb{1})}, \tag{1}$$

satisfying $UPU^\dagger = P_0$. Here, P_0 projects onto the low-energy or qubit subspace of a set of noninteracting circuits $H_0 = \sum_i H_i$, being Hi the independent Hamiltonian of each of them, and P accesses the low-energy subspace when those circuits interact producing a Hamiltonian $H = H_0 + V$. $\mathbb{1}_0$ and $\mathbb{1}$ are the projectors onto the full set of eigenstates of the Hamiltonians. For moderate interactions, the subspace P remains gapped from nonqubit states and allows us to interpret the physical interaction V as a coupling between qubits in the unperturbed qubit subspace,

$$H_{\text{eff}} = P_0 UPHPU^\dagger P_0. \tag{2}$$

Consani and Warburton[7] computed U directly from its definition (1) and showed that H_{eff} includes qubit–qubit interactions[7] not captured by perturbative methods. To make the method affordable, Consani and Warburton[7] express H in the basis of eigenstates of the uncoupled qubits with up to N_T states—a number determined by convergence. In this basis, H is approximately diagonalized to recover the interacting eigenstates and P, and U is computed using Eq. (1). This step dominates the complexity of the algorithm, due to working with matrices of size $N_T \times N_T$.

We propose to compute the rank-d matrices P_0UP and $PU^\dagger P_0$, using only the d eigenstates of H_0 and H that span their low-energy subspaces. Thus, instead of computing U in the full basis, we only need to estimate $d \times d$ matrices. The cost of the algorithm is now dominated by the calculation of the d eigenstates, a step also presents in Consani's work, which is done efficiently using Lanczos techniques. To develop this simplification, we note that P_0UP involves a rank-d transformation A,

$$P_0 UP = \sum_{i,j=1}^{d} A_{ij} |\psi_i^0\rangle\langle\psi_j| = P_0 AP, \tag{3}$$

among the basis $|\psi_j^0\rangle$ and $|\psi_j\rangle$ in which we represent P_0 and P. Using these basis, H_{eff} becomes

$$H_{\text{eff}} = \sum_{ijk=1\ldots d} |\psi_i^0\rangle A_{ij} \langle\psi_j|H|\psi_j\rangle (A^\dagger)_{jk} \langle\psi_k^0|. \tag{4}$$

We introduce a rank-d operator $B = P_0P$, such that $(P_0UP)^2 = (P_0AP)^2 = P_0AB^\dagger AP = P_0BP$; hence, $AB^\dagger A = B$ and its singular value decomposition[23] $B = W\Sigma V^\dagger$, in terms of two unitary transformations $W, V \in \mathbb{C}^{d\times d}$, and a non-negative diagonal matrix Σ. Using these matrices, we can verify that the previous equation is satisfied by $A = WV^\dagger$.

We are interested on using the SWT on pairs of superconducting qubits, with a bare Hamiltonian $H_0 = H_1 + H_2$ and an interaction γV controlled by a parameter γ. Provided that there exists a gapped low-energy subspace P, we can express the circuit model $H = H_0 + \gamma V$ in the charge basis and compute H_{eff}, which we expand in the complete basis of Pauli matrices as

$$H_{\text{eff}} = \sum_{i=x,y,z} \left(\frac{h_{1i}}{2} \sigma_1^i + \frac{h_{2i}}{2} \sigma_2^i \right) + \sum_{i,j=x,y,x} J_{ij} \sigma_1^i \sigma_2^j. \tag{5}$$

We apply this technique to 3JJQs,[17,24] which are composed of a superconducting loop interrupted by three Josephson junctions, two identical and one a factor α times smaller (cf. Fig. 1). At full frustration $\Phi_{\text{ext}} = \frac{1}{2}\Phi_0$, the periodic inductive potential has a unit cell depicted in Fig. 1(b). For $\alpha > 0.5$, this unit cell has two minima that correspond to two persistent current states flowing in opposite direction. Quantum tunneling couples these current states, creating an effective qubit subspace $H_q = \frac{\Delta}{2}\sigma^z$ with a gap Δ. We choose our qubit parameters in the range $0.6 < \alpha < 0.9$. The first inequality guarantees that the qubit subspace P_0 is gaped from nonqubit states with a large anharmonicity $E_{21} > 2\Delta$. The second inequality ensures that the intra-cell tunneling along direction d_1 dominates over the inter-cell tunneling d_2 [cf. Fig. 1(b)], reducing the sensitivity to phase slips and charge noise.[17] We also study qubits with a shunting capacitor in parallel to the small junction because, despite their reduced anharmonicity, they exhibit lower sensitivity to flux noise and better reproducibility.[25]

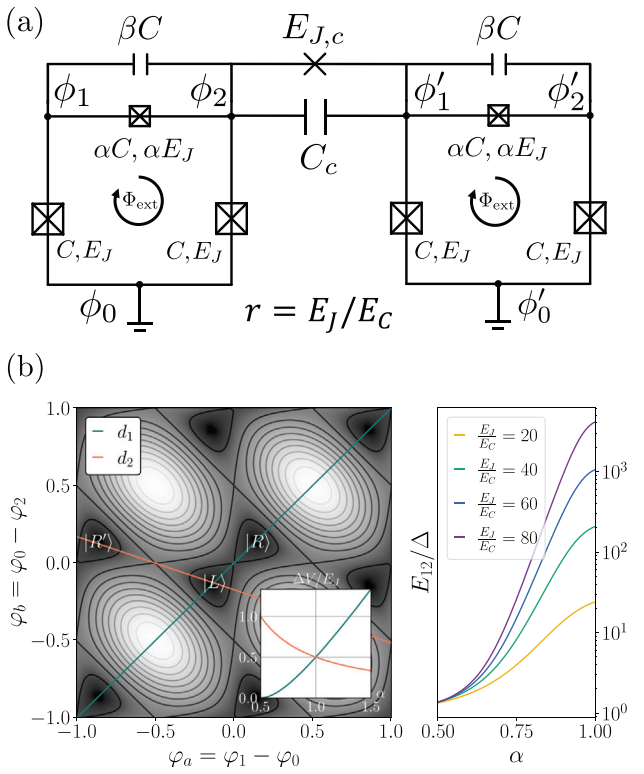

FIG. 1. (a) Two identical c-shunted 3JJQs with grounds in nodes ϕ_0 and ϕ_0' coupled through a capacitor with capacitance C_c and a Josephson junction with Josephson energy $E_{J,c}$. (b) Analysis of one single 3JJQ. At left panel, unit cell for the periodic nonlinear potential at full frustration, the potential strength is represented in a scale of colors from the maximum in white to the minimum in black, as a function of the phase variables $\varphi_i = 2\pi\phi_i/\Phi_0$. The two qubit states are indicated as $|L\rangle, |R\rangle$ for the unit cell ($|R'\rangle$ corresponds to a qubit state at an adjacent cell). The inset shows the barrier height through the intra- and inter-cell tunneling directions. Right panel: ratio of energy differences between E_{12}/Δ, with E_{12} the energy difference between second and first exited levels and Δ the qubit gap, as a function of α for multiple values of $r = E_J/E_C$ and $\beta = 0$. Notice that the relative anharmonicity is $\alpha_r = E_{12}/\Delta - 1$.

Now we move on the discussion of qubit's coupling. We consider circuits such as the one in Fig. 1(a), as well as 11 other topologies that change the places where the capacitor and inductor are attached and the positions of the grounds. These circuits are quantized and brought to the form $H = H_1 + H_2 + H_{\text{int}}$, where the $H_{1,2}$ is identified as renormalized single-qubit Hamiltonians, and the remaining interactions are grouped into a perturbation $H_{\text{int}} := \gamma V$ (see the supplementary material A). The complete Hamiltonian is then analyzed using the SWT and brought into a form (5). Working at the symmetry point, $\Phi_{\text{ext}} = \frac{1}{2}\Phi_0$, we find that the only nonzero terms are the renormalized single-qubit gaps $h_{1z} = \Delta_1$ and $h_{2z} = \Delta_2$, and the qubit–qubit interactions $\sigma_1^x\sigma_2^x$, $\sigma_1^y\sigma_2^y$, and $\sigma_1^z\sigma_2^z$, modulated by the coupling strengths J_{xx}, J_{yy}, and J_{zz}.

Let us discuss first the capacitive coupling of two identical 3JJQs shown in Fig. 1(a) with $C_c = \gamma C$, $E_{J,c} = 0$, and grounds at $\phi_0 = \phi_0' = 0$. From the analytical perturbative study performed in Ref. 19, we expect three types of interactions $\sigma_1^y\sigma_2^y$, $\sigma_1^z\sigma_2^z$, and $\sigma_1^x\sigma_2^x$, corresponding to the first, second, and third order coupling in γ. The J_{yy} terms are explained by the matrix elements of the charge operator within the qubit subspace,[19] while J_{zz} and J_{xx} are interactions mediated by states outside the qubit space. Perturbation theory agrees qualitatively with the numerically exact results shown in Fig. 2(a) for small interaction strengths γ, but its prediction fails for moderate interactions where the J_{yy} and J_{zz} couplings reach a maximum similar in magnitude and then slowly start to decay.

Figures 2(b)–2(d) display the growth of the relative interaction strength J/Δ for the design parameters in Fig. 1(a) (α, r, and β), illustrating the crossover from weak $J/\Delta \ll 1$ to strong coupling regime $J/\Delta \approx 1$. For small γ, the behavior of the coupling is dominated by the perturbative tendencies in J_{ii}. For larger couplings, the growth of J/Δ is dominated by the exponential decrease[17] of the gap $\log(\Delta) = \mathcal{O}\left(\sqrt{C_q/C}\right)$ with the renormalized qubit capacitance, which grows with γ, β, and α. This competition explains the nonmonotonical behavior found in $J_{zz}/\Delta, J_{yy}/\Delta$ with respect to α, r [cf. Figs. 2(b) and 2(c)], as J decreases while $1/\Delta$ increases with those parameters. Finally, for the limited range of γ where the gap is not negligible, J_{zz}/Δ and J_{yy}/Δ always decrease with the shunting β.

Note that at the same time as the intra-cell tunneling is suppressed, which produces the exponential decay in the qubit's gap, the tunneling along the d_2 direction may get activated, see Fig. 1. This phenomenon is due to the renormalization of the capacitances along different directions and is, thus, dependent on the qubit's parameters and the circuit topology. A consequence of this activation is the fast growth of the $J_{xx}\sigma_1^x\sigma_2^x$ interaction. This is, in our opinion, a regime to be avoided: first, because the J_{xx} can be obtained by other (inductive) means; and second, because the activation of the inter-cell tunneling is accompanied by a greater sensitivity to electrostatic field fluctuations.

Different coupling topologies produce qualitatively similar plots, although the relative coupling strength $J_{ii}/\Delta = 1$ may be reached for lower or higher values of the capacitance γ, and the relative sign of the interactions might change. We have also studied different grounding schemes. Topologically, there are two distinct combinations: We can place the grounds between the small and big junctions—i.e., $\phi_1 = 0$ or $\phi_2 = 0$—or we can place them between the big junctions $\phi_0 = \phi_{0'} = 0$. Choosing between $\phi_1 = 0$ or $\phi_2 = 0$ is equivalent to flipping the flux passing through the qubit and changes the sign of the σ^y and σ^x operators. If we choose topologically equivalent grounds for both qubits, we obtain coupling strengths with similar magnitude as the ones seen before. However, there are somewhat pathological choices—e.g., $\phi_0 = \phi_{1'} = 0$ connecting nodes 0 and 1′—where the qubits experience different renormalizations and their gaps differ as interaction grows.

It must be remarked that for all choices of connecting nodes and ground nodes, we always obtain both $J_{yy}\sigma_1^y\sigma_2^y$ and $J_{zz}\sigma_1^z\sigma_2^z$ interactions simultaneously, with very similar magnitude. This means that we can engineer effective qubit–qubit interactions of the approximate form $J(\sigma_1^z\sigma_2^z \pm \sigma_1^y\sigma_2^y)$, with $J \approx \Delta$ and with a sign that depends on the topology. This could produce a spectral signature that is similar to the one observed in Ref. 6, but without the flexibility suggested in that experimental work.

We have additionally studied the inductive coupling between two identical 3JJQs with a Josephson junction, using the circuit topology in Fig. 1(a), with $E_{J,c} = \gamma E_J$ and $C_c = 0$, but with grounds $\phi_1 = \phi_{2'} = 0$ (notice that we neglect the junction's capacitance). The interaction is so strong that around $\gamma \approx 0.1$, it produces a full hybridization of the low and high energy subspaces where we cannot isolate a qubit subspace.

Before this regime, for $0 < \gamma < 0.05$, as illustrated by Fig. 3(a), interactions are dominated by the coupling $J_{xx}\sigma_1^x\sigma_2^x$ between the effective dipolar magnetic moments of both qubits. In addition to this, we

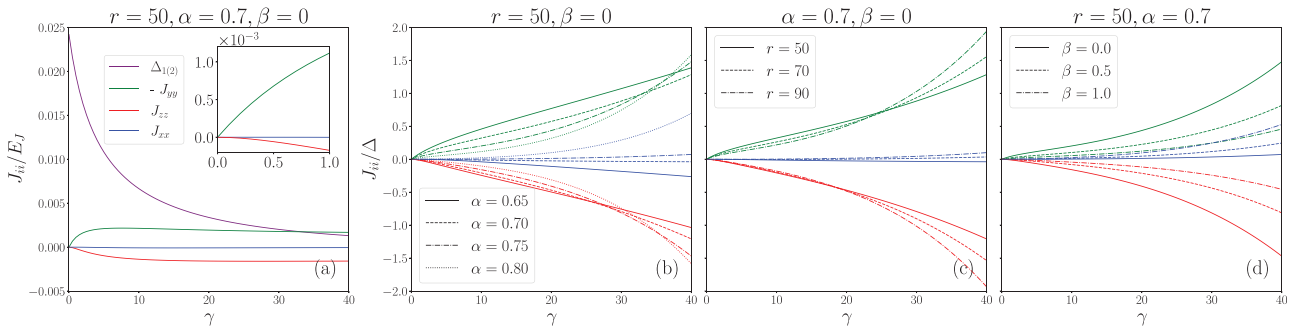

FIG. 2. Coupling strengths for two 3JJQs with ground in $\phi_0(\phi_0')$ coupled through capacitor connecting nodes $\phi_2 - \phi_1'$. (a) Effective Hamiltonian parameters as a function of γ for $\alpha = 0.70$, $r = 50$ and $\beta = 0$. (b)–(d) Ratios between the coupling strengths (J_{ii}) and the qubit gap (Δ) for fixed: (b) r and β, (c) α and β, (d) α and r. The legend in plot (a) holds for (b)–(d). We represent $-J_{yy}$ for the sake of clarity.

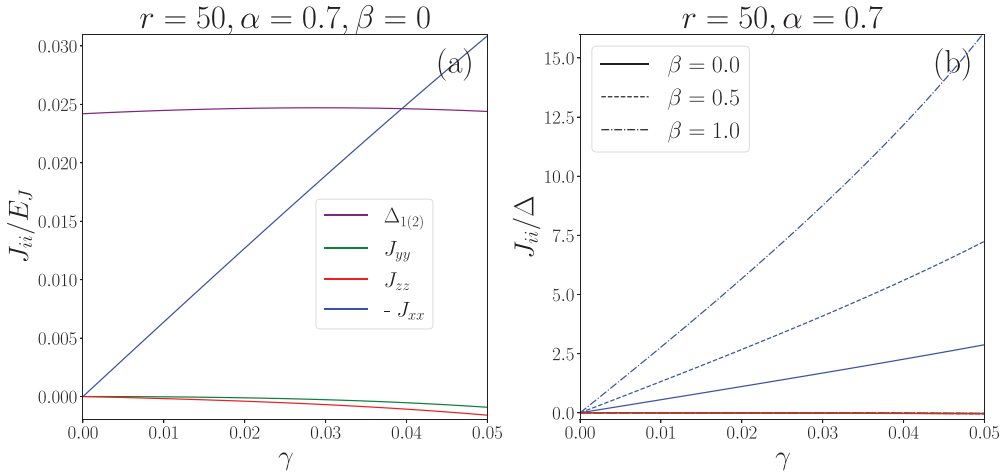

FIG. 3. Coupling strengths for two 3JJQs with ground in $\phi_1(\phi_2')$ coupled through a Josephson junction connecting nodes $\phi_2 - \phi_1'$. (a) Effective Hamiltonian parameters as a function of γ for $\alpha = 0.70$, $r = 50$ and $\beta = 0$. (b) Ratios between the coupling strengths (J_{ii}) and the qubit gap (Δ) for fixed α and r. We represent $-J_{xx}$ for the sake of clarity.

find some residual $J_{zz}\sigma_1^z\sigma_2^z$ and $J_{yy}\sigma_1^y\sigma_2^y$ contributions, which are up to three orders of magnitude weaker and can be neglected.

The dependency of the coupling strengths on the 3JJQ parameters offers a simple picture, where the dominant inductive term $J_{xx}\sigma_1^x\sigma_2^x$ grows with α and r (data not shown). This tendency is accompanied by a reduction in the qubit gap for increasing α and r. Finally, as it can be extracted from Fig. 3(b), adding a shunting capacitor to the 3JJQs reduces the qubits gap while strengthening the $\sigma_2^x\sigma_2^x$ inductive coupling. This allows for arbitrary large ratios between the coupling strength and the gap of the qubit leading to ultrastrong coupling but also favors the crossing between levels inside and outside the qubit subspace for increasingly small values of γ.

Similar to the capacitive circuit, changing the circuit topology does not affect the qualitative behavior of the interaction with the coupling strength γ. At most, the choice of coupling and ground nodes can speed up or slow down the growth of interactions with γ or change the sign of the corresponding qubit operator.

We have used dimensionless quantities $(\alpha, \beta, \gamma, r)$ in our previous analysis. We now present results using dimensional parameters close to the experimental ones in Ref. 20. Employing the machinery previously developed, we show that those parameters allow obtaining qubit–qubit strong couplings that can be implemented in experiments.

For the capacitive coupling, the parameters used in Ref. 20 are ideal to produce a Hamiltonian of the form (5) with a negligible magnetic interaction. Indeed, the small ratio between the Josephson energy and the capacitive energy ($E_C = 7.4$), $r = 35$, ensures that $J_{xx} \approx 0$ for the circuit configuration considered above, while $\alpha = 0.8$ ensures a good separation of the two-qubit subspace from higher-energy excitations, even after the coupling. However, such a large value of α gives rise to a strong renormalization of the gap, limiting the coupling constants to $J_{ii} < 0.2$ GHz, a small value for practical applications.

To overcome this limit, we propose to slightly reduce the qubit's anharmonicity, using $\alpha = 0.7$. As seen in Fig. 4(a), this modification produces effective qubit couplings $J(\sigma_1^y\sigma_2^y + \sigma_1^z\sigma_2^z)$, which are strong $(J/\Delta \approx 1)$ and values of the qubit gap and interactions that can be measured experimentally, free of thermal fluctuations. Note that models with $J(\sigma_1^y\sigma_2^y - \sigma_1^z\sigma_2^z)$ couplings are obtained by changing one of the flux threading one qubit, or the connection topology.

Figure 4(b) presents a similar analysis for the inductive coupling, using Chiorescu *et al.*'s original qubits,[20] considering both the junction and its capacitance. Since the inductive coupling between qubits is extremely strong and does not allow for large values of γ, it can be seen that the added capacitor does not really affect the coupling results. Note the lack of strong qubit renormalization allows for strong $\sigma_1^x\sigma_2^x$ coupling ($J_{xx}/\Delta > 2$) without having to modify the original qubit.

Summing up, we have performed an extensive analysis of a system composed of two 3JJQs coupled via a capacitor and a Josephson junction. This type of circuits can be implemented experimentally to produce qubits models with strong coupling in different directions. Indeed, we have obtained arbitrary interactions of the form $J^{\text{cap}}(\sigma_1^y\sigma_2^y \pm \sigma_1^z\sigma_2^z) + (J_{xx}^{\text{cap}} + J_{xx}^{\text{JJ}})\sigma_1^x\sigma_2^x$.

Our results confirm the idea that flux qubits may be used to simulate strong nonstoquastic spin Hamiltonians, but also reveal that not all interactions are independent as found by the simultaneous appearance of $\sigma_1^y\sigma_2^y$ and $\sigma_1^z\sigma_2^z$ terms. This may have consequences for the interpretation of works that argue the classical simulability of superconducting quantum circuits.[26,27]

Out of the two interactions studied, J_{xx}^{JJ} admits straightforward tunability, replacing the junction with a dc-SQUID. We believe that this avoids the complex dynamic of the usual rf-SQUID tunable couplers, lifting its geometric constrains.[6,7,28–30] We also believe that the capacitive interactions J^{cap} can be tuned with the help of mediating circuits, such as capacitively connected, tunable frequency qubits, and resonators.

Designing the type of circuits discussed here is a difficult task. A source of problems is the nonlinear dependence of physical quantities on the design parameters, as the exponential renormalization of the qubit gap with the coupling capacitance. Our methods could help experimentalists in the design and optimization of qubits and couplers. As an example of the utility of our work, we have found acceptable parameters close to earlier experimental setups, which provide strong capacitively or inductively coupled qubits.

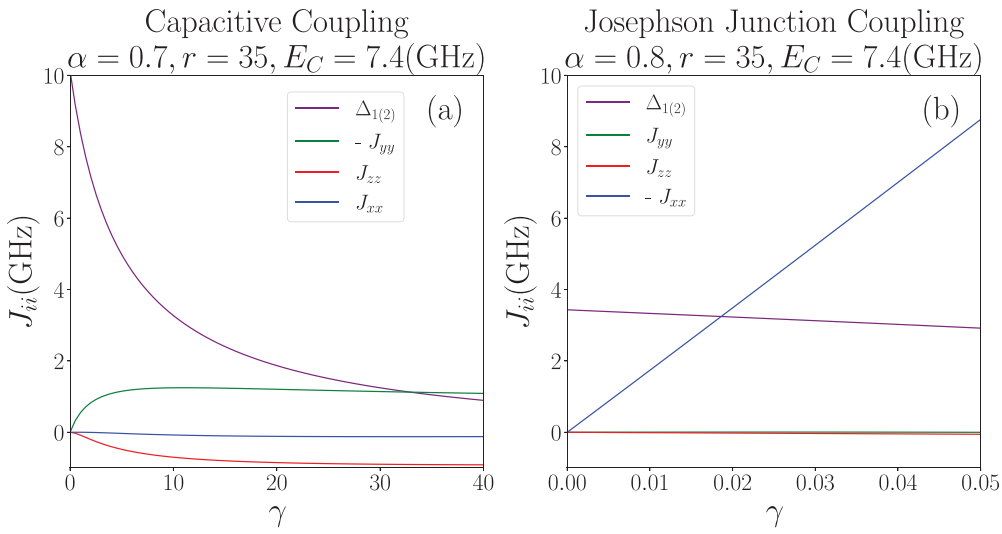

FIG. 4. Coupling strengths for the reference circuits using real experimental 3JJQs parameters.[20] (a) Effective Hamiltonian parameters as a function of γ for $\alpha = 0.70$, $r = 35$, $E_C = 7.4$ (GHz), and $\beta = 0$ for the capacitive coupling. (b) Effective Hamiltonian parameters as a function of γ for $\alpha = 0.80$, $r = 35$, $E_C = 7.4$ (GHz), and $\beta = 0$ for the Josephson junction coupling (including the capacitor that accompanies it). We represent $-J_{yy}$ in (a) and $-J_{xx}$ in (b) for the sake of clarity.

Additionally, we have developed an improved numerical scheme to derive effective Hamiltonians of coupled quantum systems, reducing the complexity of the original algorithm in Ref. 7 down to the size of the computational space under analysis, times the size for the representation of the relevant eigenstates. This allows us to treat a wider class of models, such as qubits interacting with resonators,[19] and can be extended to treat larger systems if a clever representation—e.g., tensor networks—is used to describe the low-energy states. This way, we expect to scale our simulations up to four or five qubits, exploring the gap renormalization due to capacitive couplings, and whether the effective models can still be obtained as a sum of two- or at most three-body operators in the case of strong qubit interactions.

Finally, our work leaves open questions, such as the application of our coupling scheme in the context of quantum computation, where the tunability of the capacitive couplings may become relevant. We expect to analyze this question in future works, inducing a mediated capacitive coupling via, for instance, microwave resonators[19] or other qubits.[9]

See the supplementary material for the full derivation of the system's Hamiltonian (supplementary material A) and a further study of the multiple circuit configurations (supplementary material B).

This work has been supported by European Commission FET-Open project AVaQus Grant Agreement 899561 and CSIC Quantum Technologies Platform PTI-001. Financial support by Fundación General CSIC (Programa Comfuturo) is acknowledged. The numerical computations have been performed in the cluster Trueno of the CSIC.

AUTHOR DECLARATIONS

Conflict of Interest

The authors have no conflicts to disclose.

DATA AVAILABILITY

The data that support the findings of this study are available from the corresponding author upon reasonable request.

REFERENCES

[1]M. A. Nielsen and I. L. Chuang, *Quantum Computation and Quantum Information: 10th Anniversary Edition* (Cambridge University Press, 2010).
[2]I. Buluta and F. Nori, Science **326**, 108 (2009).
[3]J. Cirac and P. Zoller, Nat. Phys. **8**, 264 (2012).
[4]D. Ballester, G. Romero, J. J. García-Ripoll, F. Deppe, and E. Solano, Phys. Rev. X **2**, 021007 (2012).
[5]M. C. Collodo, J. Herrmann, N. Lacroix, C. K. Andersen, A. Remm, S. Lazar, J.-C. Besse, T. Walter, A. Wallraff, and C. Eichler, Phys. Rev. Lett. **125**, 240502 (2020).
[6]I. Ozfidan, C. Deng, A. Smirnov, T. Lanting, R. Harris, L. Swenson, J. Whittaker, F. Altomare, M. Babcock, C. Baron, A. Berkley, K. Boothby, H. Christiani, P. Bunyk, C. Enderud, B. Evert, M. Hager, A. Hajda, J. Hilton, S. Huang, E. Hoskinson, M. Johnson, K. Jooya, E. Ladizinsky, N. Ladizinsky, R. Li, A. MacDonald, D. Marsden, G. Marsden, T. Medina, R. Molavi, R. Neufeld, M. Nissen, M. Norouzpour, T. Oh, I. Pavlov, I. Perminov, G. Poulin-Lamarre, M. Reis, T. Prescott, C. Rich, Y. Sato, G. Sterling, N. Tsai, M. Volkmann, W. Wilkinson, J. Yao, and M. Amin, Phys. Rev. Appl. **13**, 034037 (2020).
[7]G. Consani and P. A. Warburton, New J. Phys. **22**, 053040 (2020).
[8]A. J. Kerman, New J. Phys. **21**, 073030 (2019).
[9]F. Arute, K. Arya, R. Babbush, D. Bacon, J. C. Bardin, R. Barends, R. Biswas, S. Boixo, F. G. S. L. Brandao, D. A. Buell, B. Burkett, Y. Chen, Z. Chen, B. Chiaro, R. Collins, W. Courtney, A. Dunsworth, E. Farhi, B. Foxen, A. Fowler, C. Gidney, M. Giustina, R. Graff, K. Guerin, S. Habegger, M. Harrigan, M. J. Hartmann, A. Ho, M. Hoffmann, T. Huang, T. S. Humble, S. V. Isakov, E. Jeffrey, Z. Jiang, D. Kafri, K. Kechedzhi, J. Kelly, P. V. Klimov, S. Knysh, A. Korotkov, F. Kostritsa, D. Landhuis, M. Lindmark, E. Lucero, D. Lyakh, S. Mandrà, J. R. McClean, M. McEwen, A. Megrant, X. Mi, K. Michielsen, M. Mohseni, J. Mutus, O. Naaman, M. Neeley, C. Neill, M. Yuezhen Niu, E. Ostby, A. Petukhov, J. C. Platt, C. Quintana, E. G. Rieffel, P. Roushan, N. C. Rubin, D. Sank, K. J. Satzinger, V. Smelyanskiy, K. J. Sung, M. D. Trevithick, A. Vainsencher, B. Villalonga, T. White, Z. J. Yao, P. Yeh, A. Zalcman, and H. Neven, Nature **574**, 505 (2019).

[10]S. Bravyi, D. P. Divincenzo, R. Oliveira, and B. M. Terhal, Quantum Inf. Comput. **8**, 361 (2008).
[11]Y. Susa, J. F. Jadebeck, and H. Nishimori, Phys. Rev. A **95**, 042321 (2017).
[12]T. Albash, Phys. Rev. A **99**, 042334 (2019).
[13]L. Hormozi, E. W. Brown, G. Carleo, and M. Troyer, Phys. Rev. B **95**, 184416 (2017).
[14]T. Albash and D. A. Lidar, Rev. Mod. Phys. **90**, 015002 (2018).
[15]J. Kempe, A. Kitaev, and O. Regev, SIAM J. Comput. **35**, 1070 (2006).
[16]R. Oliveira and B. M. Terhal, Quantum Inf. Comput. **8**, 900–924 (2008).
[17]T. P. Orlando, J. E. Mooij, L. Tian, C. H. van der Wal, L. S. Levitov, S. Lloyd, and J. J. Mazo, Phys. Rev. B **60**, 15398 (1999).
[18]T. Satoh, Y. Matsuzaki, K. Kakuyanagi, K. Semba, H. Yamaguchi, and S. Saito, "Ising interaction between capacitively-coupled superconducting flux qubits," arXiv:1501.07739 (2015).
[19]M. Hita-Pérez, G. Jaumà, M. Pino, and J. J. García-Ripoll, "Ultrastrong capacitive coupling of flux qubits," arXiv:2108.02549 (2021).
[20]I. Chiorescu, Y. Nakamura, C. J. P. M. Harmans, and J. E. Mooij, Science **299**, 1869 (2003).
[21]J. R. Schrieffer and P. A. Wolff, Phys. Rev. **149**, 491 (1966).
[22]S. Bravyi, D. P. DiVincenzo, and D. Loss, Ann. Phys. **326**, 2793 (2011).
[23]G. H. Golub and C. F. Van Loan, *Matrix Computations*, 3rd ed. (Johns Hopkins University Press, Baltimore, 1996).
[24]C. H. van der Wal, A. C. J. ter Haar, F. K. Wilhelm, R. N. Schouten, C. J. P. M. Harmans, T. P. Orlando, S. Lloyd, and J. E. Mooij, Science **290**, 773 (2000).
[25]F. Yan, S. Gustavsson, A. Kamal, J. Birenbaum, A. P. Sears, D. Hover, T. J. Gudmundsen, D. Rosenberg, G. Samach, S. Weber *et al.*, Nat. Commun. **7**(1), 12964 (2016).
[26]A. Ciani and B. M. Terhal, Phys. Rev. A **103**, 042401 (2021).
[27]T. Halverson, L. Gupta, M. Goldstein, and I. Hen, "Efficient simulation of so-called non-stoquastic superconducting flux circuits," arXiv:2011.03831 (2020).
[28]D. Kafri, C. Quintana, Y. Chen, A. Shabani, J. M. Martinis, and H. Neven, Phys. Rev. A **95**, 052333 (2017).
[29]S. J. Weber, G. O. Samach, D. Hover, S. Gustavsson, D. K. Kim, A. Melville, D. Rosenberg, A. P. Sears, F. Yan, J. L. Yoder *et al.*, Phys. Rev. Appl. **8**, 014004 (2017).
[30]M. S. Allman, F. Altomare, J. D. Whittaker, K. Cicak, D. Li, A. Sirois, J. Strong, J. D. Teufel, and R. W. Simmonds, Phys. Rev. Lett. **104**, 177004 (2010).